

NUMERICAL STUDY OF LIQUID INTERNAL CIRCULATION DURING DROPLET-STREAM COMBUSTION

Edson G. Moreira Filho

Albino J.K. Leiroz[♦]

Department of Mechanical and Materials Engineering

Instituto Militar de Engenharia

22290-270 -- Rio de Janeiro – RJ

E-mail: leiroz@ime.eb.br

Abstract

A numerical study of interference effects within the liquid-phase of an infinite linear array of spherical droplets in the absence of surrounding convective effects is discussed in the present work. The transient evolution of the flow field, obtained using a vorticity-stream function approach, show the development of two toroidal vortices surrounded by a viscous boundary layers close the liquid-gas interface and by a internal wake in the stream axis region. The evolution of the temperature field is also analyzed. Results indicate that velocity and temperature distributions inside individual stream droplets are significantly different from patterns found for isolated droplets in convective streams.

Keywords: Droplet Combustion, Droplet Vaporization, Numerical Methods, Convection.

1. INTRODUCTION

The atomization of liquid fuel jets, which usually precede the vaporization and combustion in a wide range of important technological applications, invariably leads to sprays with a large droplet volumetric fraction. Within these dense sprays, interaction effects and deviations from the isolated droplet behavior (Spalding, 1953; 1955) become significant and the multi-dimensionality of the phenomena make pure analytical treatments not applicable.

Reviews of numerical studies of multi-droplet combustion have been presented covering a broad selection of physical situations and stressing the importance of droplet interaction (Sirignano, 1993, Annamalai, 1992). Numerical studies share the compromise of addressing the different spatial and time scales present in the multi-droplet combustion phenomena and are usually limited to arrays with a small number of droplets.

The droplet interaction phenomena can be understood from the nature of the involved physical process. Energy in the form of heat diffuses and convects from the surrounding ambience or reaction zone to the droplet surface, increasing the liquid droplet temperature and leading to phase-change. Mass diffusion is also present due to species concentration gradients. In a combustion situation, the vaporized liquid is transported to the flame (Stefan Flow) where reaction occurs and heat is released to the ambient and to the condensed phase. Interdroplet

[♦] Author to whom correspondence should be addressed. e-mail: *leiroz@ime.eb.br*

effects alter the manner in which an individual droplet receives heat and thus affect its heating and vaporization. In reacting situations, competition for the ambient oxidant affects the flame position and shape, and variations in ignition delays become influenced by the spray denseness.

Liquid circulation studies for isolated droplets in convective stream show the development of a single toroidal vortex surrounded by a viscous boundary layer and an internal wake (Prakash & Sirignano, 1978). Liquid vaporization effects are initially neglected. Results are used to correlate the vortex strength to the shear stress at the liquid-gas interface. Energy diffusion within the recirculation zone is also shown to follow a one-dimensional behavior due to the circulatory flow pattern. For vaporizing liquid droplets, an integral approach is used in the analysis of viscous, thermal and species boundary layers (Prakash & Sirignano, 1980). Results show the importance of transient effects and that the temperature distribution within the discrete phase is nonuniform during the droplet lifetime.

A detailed numerical analysis of a spherical droplet suspended by a thin filament in a convective stream (Shih & Megaridis, 1995). The filament suspended droplet is a typical setup for reactive and nonreactive experimental studies. Results show the influence of the filament on the general liquid internal circulation, which includes the development of secondary vortices. Besides, significant effects of the circulation patterns on the droplet vaporization rate were observed.

In the absence of convective effects, droplet mass vaporization reduction in linear reacting arrays due to interference was found and correlated to interdroplet spacing (Leiroz & Rangel, 1995a; 1995b). Furthermore, the nonconvective quasi-steady results indicate the potential flow solution as a valid approximation for the viscous velocity field, based on a negligible tangential velocity observed along the droplet surface. The droplet surface blowing velocity was found to vary along the liquid-gas interface leading to the observed negligible tangential velocity.

Gas-phase transient results during droplet stream combustion have shown the existence of non-vanishing droplet surface tangential velocities that can lead to shear-induced liquid motion within the dispersed phase (Leiroz, 1996). Nevertheless, similarly to the quasi-steady case, the droplet surface normal velocity was found to vary along the liquid-gas interface. Besides, preferential vaporization near the droplet equatorial plane, that can also induce liquid movement inside the droplet, was also observed. Results also show, for the time intervals investigated, a weak dependence of the droplet mass vaporization rate on the interdroplet spacing.

The transient motion of liquid inside spherical droplets generated by the presence of significant interference effects in droplet streams under stagnant environment conditions is numerically investigated. Constant thermophysical properties and quasi-steady conditions are assumed for the purpose of the calculations. Preferential vaporization effects are also neglected for the present work. The transient energy and momentum governing equations, written in vorticity-stream function formulation, are discretized using the BTCS Finite Difference scheme (Hoffman, 1992). Results show the temporal evolution of the flow and temperature fields, which are also compared with patterns found in isolated droplet in convective conditions.

2. ANALYSIS

In the absence of external convective effects, the study of interactive effects within the dispersed phase of an infinitely long linear array of spherical equidistant droplets, shown in Fig.1a can be performed in the solution domain depicted in Fig.1b. Symmetry considerations around the droplet stream axis, the droplet equatorial plane and the interdroplet mean distance plane are explored in the simplification of the solution domain.

The flow and energy governing equations are written in nondimensional form, assuming constant thermophysical properties, negligible body forces and secondary convective effects, as

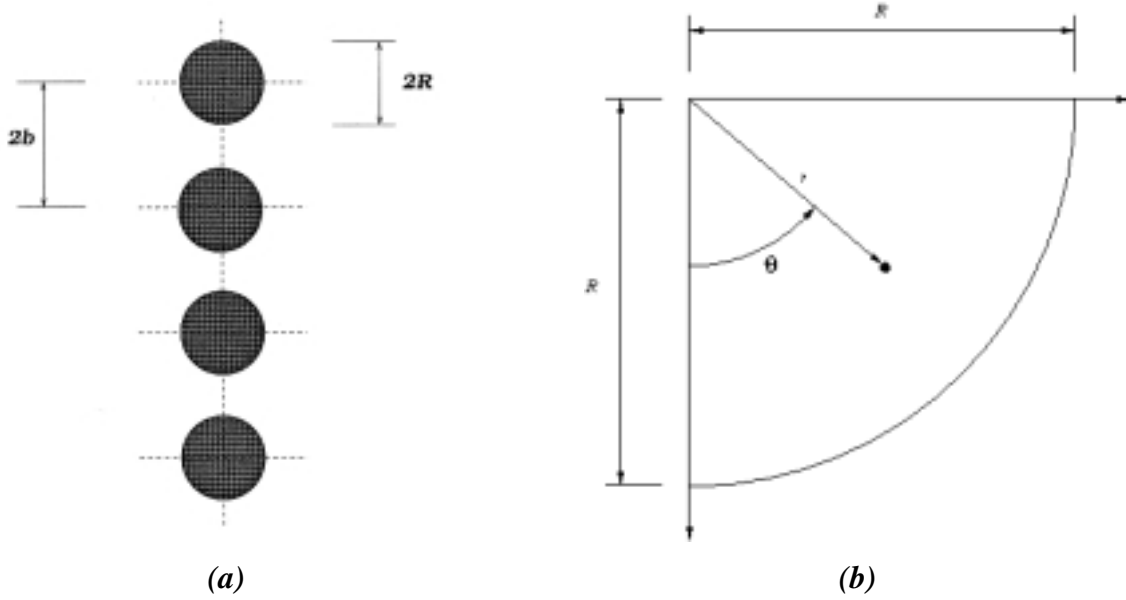


Figure 1. Sketch of the center portion of an infinite stream of droplets (a) and physical domain and principal dimensions (b)

$$\frac{1}{r^2} \frac{\partial}{\partial r} (r^2 u_r) + \frac{1}{r \sin \theta} \frac{\partial}{\partial \theta} (u_\theta \sin \theta) = 0 \quad (1)$$

$$\begin{aligned} \frac{\partial u_r}{\partial t} + u_r \frac{\partial u_r}{\partial r} + \frac{u_\theta}{r} \frac{\partial u_r}{\partial \theta} - \frac{u_\theta^2}{r} = -\frac{\partial p}{\partial r} + \\ \frac{1}{Re} \left[\frac{1}{r^2} \frac{\partial^2}{\partial r^2} (r^2 u_r) + \frac{1}{r^2 \sin \theta} \frac{\partial}{\partial \theta} \left(\sin \theta \frac{\partial u_r}{\partial \theta} \right) \right] \end{aligned} \quad (2)$$

$$\begin{aligned} \frac{\partial u_\theta}{\partial t} + u_r \frac{\partial u_\theta}{\partial r} + \frac{u_\theta}{r} \frac{\partial u_\theta}{\partial \theta} + \frac{u_\theta u_r}{r} = -\frac{1}{r} \frac{\partial p}{\partial \theta} + \\ \frac{1}{Re} \left[\frac{1}{r^2} \frac{\partial}{\partial r} \left(r^2 \frac{\partial u_\theta}{\partial r} \right) + \frac{1}{r^2} \frac{\partial}{\partial \theta} \left(\frac{1}{\sin \theta} \frac{\partial (u_\theta \sin \theta)}{\partial \theta} \right) + \frac{2}{r^2} \frac{\partial u_r}{\partial \theta} \right] \end{aligned} \quad (3)$$

$$\frac{\partial T}{\partial t} + u_r \frac{\partial T}{\partial r} + \frac{u_\theta}{r} \frac{\partial T}{\partial \theta} = \frac{1}{Pe} \left\{ \frac{1}{r^2} \frac{\partial}{\partial r} \left(r^2 \frac{\partial T}{\partial r} \right) + \frac{1}{r^2 \sin \theta} \frac{\partial}{\partial \theta} \left(\sin \theta \frac{\partial T}{\partial \theta} \right) \right\} \quad (4)$$

with boundary conditions

$$u_\theta = u_{\theta,s}(\theta), \quad u_r = 0, \quad T = 1; \quad r = 1, \quad 0 < \theta < \pi/2 \quad (5)$$

$$u_\theta = 0, \quad \frac{\partial u_r}{\partial \theta} = 0, \quad \frac{\partial T}{\partial \theta} = 0; \quad \theta = 0, \quad 0 \leq r \leq 1 \quad (6)$$

$$u_\theta = 0, \quad \frac{\partial u_r}{\partial \theta} = 0, \quad \frac{\partial T}{\partial \theta} = 0; \quad \theta = \pi/2, \quad 0 \leq r \leq 1 \quad (7)$$

and initial conditions

$$u_\theta = 0, u_r = 0, T = 0; 0 \leq r \leq 1, 0 \leq \theta \leq \pi/2 \quad (8)$$

which corresponds to the instantaneous injection of the droplet stream into a surrounding gas environment.

The nondimensional variables in Eqs. 1-8 are defined as

$$r = \frac{r^*}{R}; u_\theta = \frac{u_\theta^*}{u_{s,max}^*}; u_r = \frac{u_r^*}{u_{s,max}^*}; p = \frac{p^*}{\rho (u_{s,max}^*)^2}; t = \frac{t^*}{R/u_{s,max}^*}; T = \frac{T^* - T_0^*}{T_s^* - T_0^*} \quad (9)$$

where the droplet radius (R) and the maximum tangential velocity along the droplet surface ($u_{s,max}^*$) are used as length and velocity characteristic quantities, respectively.

According to the nondimensional variables defined in Eq. 9, the Reynolds (Re), Prandtl (Pr) and Peclet (Pe) numbers are defined as

$$Re = \frac{u_{s,max}^* R}{\nu}; Pr = \frac{\nu}{\alpha}; Pe = Re \cdot Pr \quad (10)$$

where ν and α represent the kinematic viscosity and the thermal diffusivity, respectively.

In order to decouple the pressure and velocity fields and reduce the number of equations necessary for the flow analysis, the primitive variable formulation described by Eqs. 1-3 are rewritten in vorticity-stream function form as

$$\frac{\partial \xi_\phi}{\partial t} + u_r \frac{\partial \xi_\phi}{\partial r} + \frac{u_\theta}{r} \frac{\partial \xi_\phi}{\partial \theta} = \frac{\xi_\phi}{r} (u_r + u_\theta \cot \theta) + \frac{1}{Re} \left\{ \frac{1}{r^2} \frac{\partial}{\partial r} \left(r^2 \frac{\partial \xi_\phi}{\partial r} \right) + \frac{1}{r^2} \frac{\partial}{\partial \theta} \left[\frac{1}{\sin \theta} \frac{\partial}{\partial \theta} (\xi_\phi \sin \theta) \right] \right\} \quad (11)$$

$$-\xi_\phi = \frac{1}{r^2 \sin \theta} \frac{\partial}{\partial r} \left[r^2 \frac{\partial}{\partial r} \left(\frac{\psi}{r} \right) \right] - \frac{1}{r^3} \frac{\partial}{\partial \theta} \left[\frac{1}{\sin \theta} \frac{\partial \psi}{\partial \theta} \right] \quad (12)$$

with boundary conditions

$$\psi = 0; r = 1, 0 < \theta < \pi/2 \quad (13)$$

$$\psi = 0, \xi_\phi = 0; \theta = 0, 0 \leq r \leq 1 \quad (14)$$

$$\psi = 0, \xi_\phi = 0; \theta = \pi/2, 0 \leq r \leq 1 \quad (15)$$

and initial conditions

$$\psi = 0, \xi = 0; 0 \leq r \leq 1, 0 < \theta < \pi/2 \quad (16)$$

Vorticity (ξ_ϕ) and stream function (ψ) are respectively defined by the radial and tangential velocity components as

$$\xi_\phi = \frac{1}{r} \frac{\partial}{\partial r}(ru_\theta) - \frac{1}{r} \frac{\partial u_r}{\partial \theta} \quad (17)$$

and

$$u_r = \frac{1}{r^2 \sin\theta} \frac{\partial \psi}{\partial \theta}; \quad u_\theta = -\frac{1}{r \sin\theta} \frac{\partial \psi}{\partial r} \quad (18)$$

The vorticity value at the liquid-gas interface is initially unknown and is determined by an iterative solution procedure of Eqs.10-15, which also accounts for the treatment of the non-linear terms present in Eq.10.

3. NUMERICAL CONSIDERATIONS

In order to improve solution convergence and control computational costs, clustering of points in the radial direction close to the liquid-gas interface is introduced. The clustering of points is motivated by the high solution gradients expected close to the droplet surface. During the grid generation procedure, an analytical transformation expressed by (Anderson *et al.*, 1984)

$$\eta = 1 + \frac{1}{\tau} \sinh^{-1} [(r-1)\sinh(\tau)] \quad (19)$$

is applied, where the clustering parameter τ allows the control of the radial point distribution. Analytically obtained metrics are used to rewrite Eqs. 4, 11 and 12, using the introduced transformed variable η .

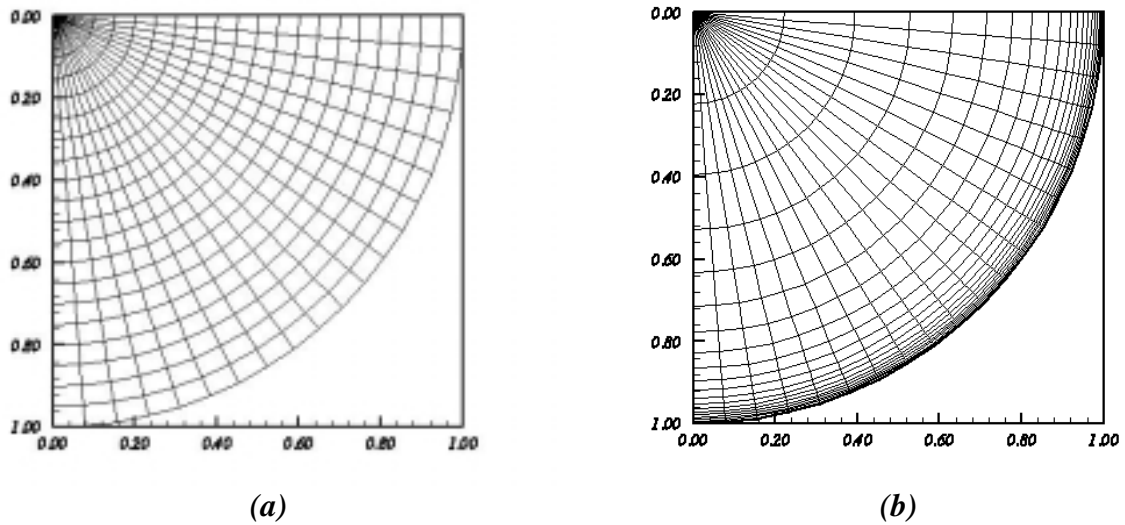


Figure 2: Discretizing grid in the physical domain for $\tau \rightarrow 0$ (a), and $\tau = 5$ (b) - 21×21 points

The transformed equations are discretized into algebraic form using a BTCS Finite-Difference scheme (Anderson *et al.*, 1984). The resulting system of algebraic equation is solved by iterative methods with local error control. Once convergence is achieved, Eq.19 is analytically inverted and solution profiles within the physical domain are obtained. Discretizing grids within the physical domain are depicted in Fig.2 for different values of the clustering parameter. As shown in Fig.2a, regularly spaced grids are recovered for vanishing clustering parameter values. For the present work, tangential droplet surface velocity components functional dependence on the angular position is obtained from gas-phase transient calculations (Leiroz, 1996).

4. RESULTS

The developed numerical procedure was initially validated for the limiting case of an isolated droplet for which the transient droplet surface velocity induced by interference vanishes. An analytical solution for the energy equation is obtained neglecting the convective terms. A convergence study is also performed in order to calibrate the mesh parameter τ . For the present work, results are shown for the case of $Re = 100$, $Pr = 1$, and $u_{\theta,s} = \sin(2\theta)$. Simulations were conducted in a 41×41 discretizing grid with a clustering parameter (τ) equal to 1.5 and $\Delta t = 10^{-7}$ which allows a 3-digit precision on the depicted results.

Stream-function transient and steady-state results shown in Fig.3 indicate the existence of two toroidal vortices within the liquid phase separated by the droplet equatorial plane. The vortex center is shown to dislocate towards to droplet equatorial plane as the flow field develops to steady-state. The existence of a boundary layer close to the liquid-gas interface and of a wake between the vortex and the droplet stream axis is also observed. Although these structures are also present in the flow pattern found for isolated droplets in convective stream (Prakash & Sirignano, 1978), the calculated two-vortex pattern is significantly different from the single vortex found for that configuration. Also, results can be used to quantify the vortex strength. The liquid motion effect on the droplet stream transport mechanisms is currently under study.

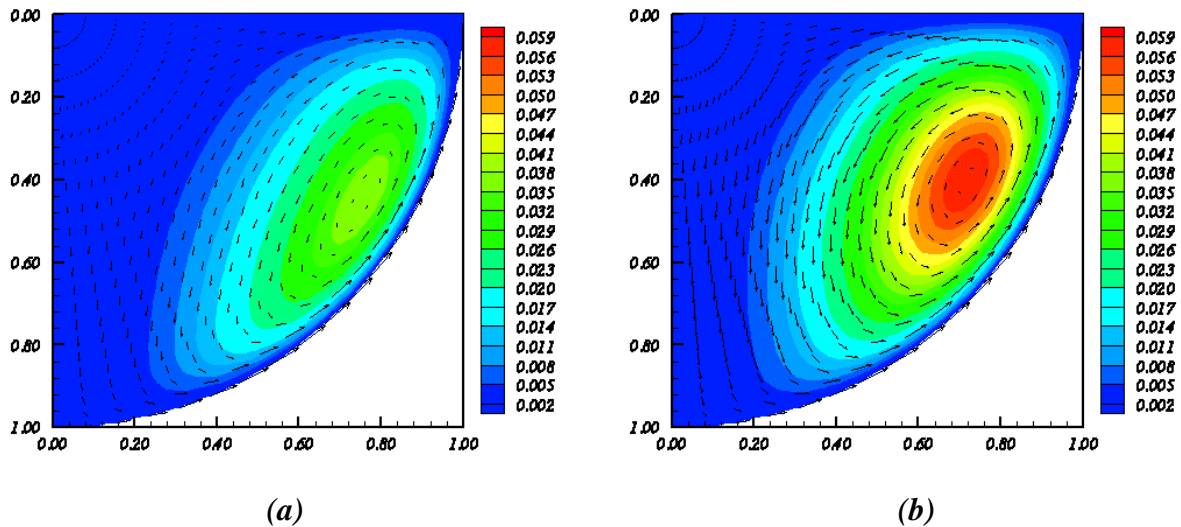


Figure 3. Transient flow $t = 0.05$ (a) and $t = 0.92$ (b) pattern showing stream-function distribution and velocity vectors. 41×41 Point Grid. $u_{\theta,s} = \sin(2\theta)$

The evolutions of the temperature and velocity fields are depicted in Fig.4. For initial times, the temperature field presents a weak dependence on the angular position within the liquid droplet as shown in Fig.4a for $t = 0.05$. Although, the almost diffusive behavior is associated with early stages of the flow development, a broadening of the thermal boundary layer close to the droplet equatorial plane is observed. For later times, convective effects become important and the temperature field deviates from the quasi-radial profile. Figure 4b, in which the temperature field is depicted for $t = 0.30$, shows that, for similar radial positions, higher temperatures can be observed closer to the droplet equatorial plane than to the stream axis. The inward motion of fluid observed as θ approach $\pi/2$ is responsible for the preferential temperature field development. An early stage of the development of the temperature field within the vortex is also shown on Fig.4b. The thermal development near the stream axis follows, as shown in Fig.4c for $t = 0.60$. It is noteworthy the non-monotonic character of the temperature field in the region, indicating a weak influence of the heat flux from droplet surface on the thermal development. A temperature field close to the trivial uniform steady solution is depicted in Fig.4d for $t = 0.90$. Due to the small velocities near the droplet center, heat diffusion becomes an important mechanism for the latter stages of the temperature field development.

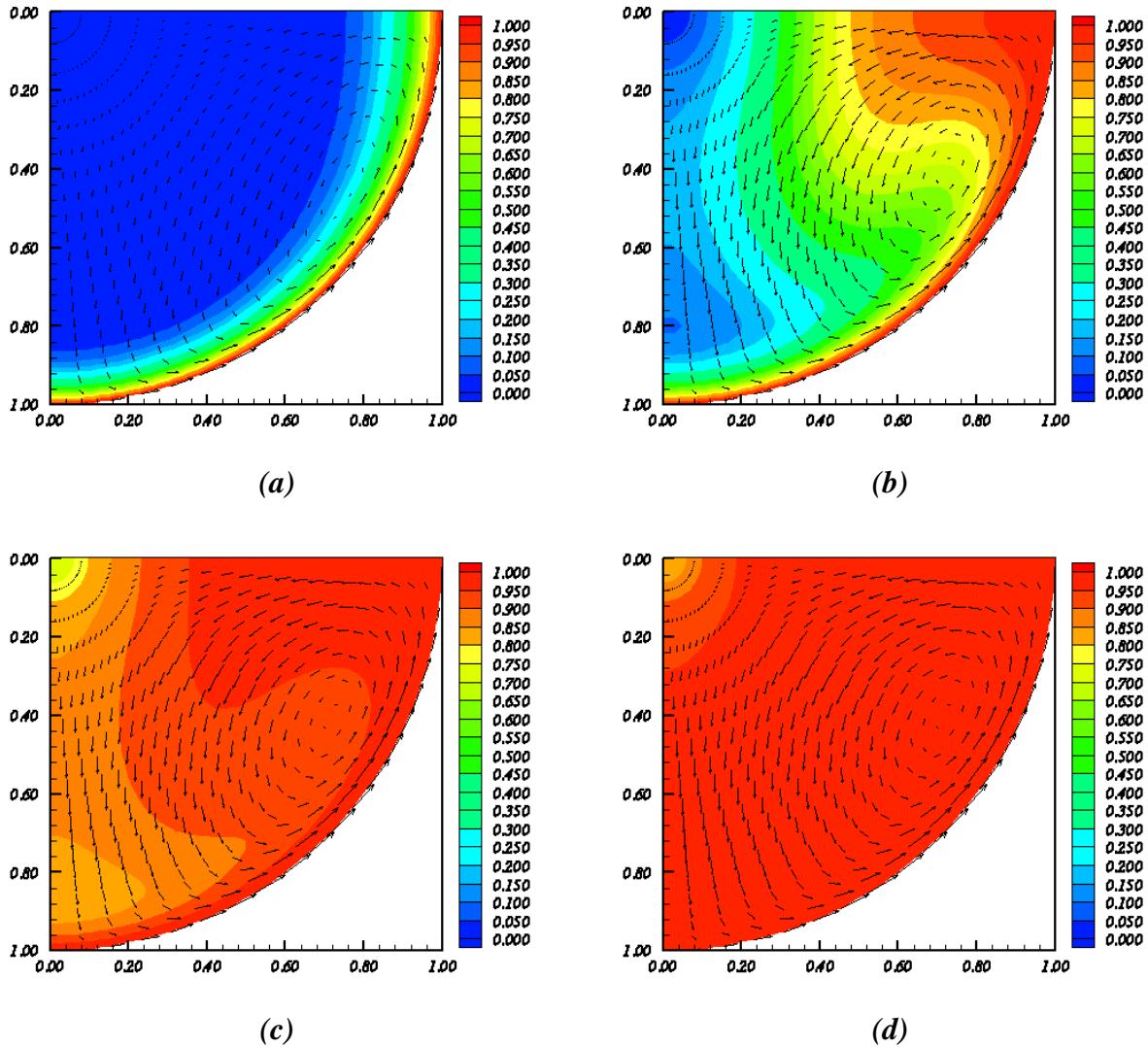


Figure 4. Temporal variation of the temperature field showing the velocity vectors for $t = 0.05$ (a), $t = 0.30$ (b), $t = 0.60$ (c) and $t = 0.90$ (d) - 41×41 Grid Points. $u_{\theta,s} = \sin(2\theta)$

5. CONCLUSIONS

The numerical analysis of the transient convective effects inside liquid droplets in a linear infinite array was performed. Results, which show the importance of transient effects, are used to draw qualitative results of the flow and temperature development characteristics. The existence and development of two toroidal vortices, which contrasts with the single vortex structure found for isolated droplet in convective streams, is shown to have a strong effect on the temperature field development. The droplet heating is shown to be governed by diffusion during the early and latter stages of the process, while convection becomes important for intermediate time intervals. Further studies are necessary to investigate the influence of the involved parameters on the flow and temperature field developments and to quantify the observed phenomena. Besides, the influence of the droplet vaporization and the consequential liquid-gas interface regression can have influence on the droplet heating process and should be investigated

6. ACKNOWLEDGMENT

The authors would like to acknowledge the financial support provided by the CNPq (Grant No. 520315/98-7). Computer resources were allocated by the Aerodynamics and Thermosciences Laboratory of the *Instituto Militar de Engenharia*.

7. REFERENCES

- Anderson, D. A., Tannehill, J. C. and Pletcher, Richard H., "Computational Fluid Mechanics and Heat Transfer", Hemisphere Publishing Corporation, 1984
- Annamalai, K.; "Interactive Process in Gasification and Combustion. Part I: Liquid Drop Arrays and Clouds", Progress Energy Combust. Science, Vol.18, pp.221-295, 1992.
- Hoffman, J. D., "Numerical Methods for Engineers and Scientists", McGraw-Hill, 1992.
- Leiroz, A.J.K. and Rangel, R.H., "Numerical Study of Droplet-Stream Vaporization at Zero-Reynolds Number", Numerical Heat Transfer, Applications, Vol.27, pp.273-296, 1995.
- Leiroz, A.J.K. and Rangel, R.H., "Interference Effects on Droplet Stream Combustion", Proc. 8th Int. Symp. on Transport. Phenomena in Combustion, San Francisco, 1995.
- Leiroz, A.J.K., "Numerical Study of Droplet-Stream Vaporization and Combustion", Ph.D. Dissertation, University of California, Irvine, 1996.
- Prakash S. and Sirignano W.A., "Liquid Fuel Droplet Heating with Internal Circulation", Int. Journal of Heat and Mass Transfer, Vol.21, 885-895, 1978
- Prakash S. and Sirignano W.A., "Theory of Convective Droplet Vaporization with Unsteady Heat Transfer in the Circulating Liquid Phase", Int. Journal of Heat and Mass Transfer, Vol.23, 253-268, 1980.
- Shih A.T. and Megaridis C.M., "Suspended Droplet Evaporation Modeling in a Laminar Convective Environment", Combustion and Flame, Vol. 102, pp. 256-270, 1995.
- Sirignano, W.A., "Fluid Dynamics of Sprays", Journal of Fluids Engineering., Vol.115, pp.345-378, 1993.
- Spalding, D.B., "The Combustion of Liquid Fuels", Proc. 4th International Symposium of Combustion, Cambridge, MA, pp. 847-864, Williams and Wilkins, Baltimore, 1953.
- Spalding, D.B., "Some Fundamentals of Combustion", Butterworths, London, 1955.